Journal of Cleaner Production 206 (2019) 251–266

Contents lists available at ScienceDirect

Journal of Cleaner Production

journal homepage: www.elsevier.com/locate/jclepro

Analyzing the trade-off between CO_2 emissions and passenger service level in the airline industry: Mathematical modeling and constructive heuristic

Mahdi Jalalian, Saiedeh Gholami*, Reza Ramezanian

Department of Industrial Engineering, K. N. Toosi University of Technology, Tehran, Iran

ARTICLE INFO

Article history:
Received 13 December 2017
Received in revised form
27 August 2018
Accepted 16 September 2018
Available online 21 September 2018

Keywords:
Flight scheduling
Green transportation
CO_2 emissions
Cruise speed control
Passenger service level
Constructive heuristic

ABSTRACT

The negative appraisals of the impact of airline industry on climate change have forced the industry to become greener. Over the past several decades, CO_2 emissions in the airline industry have increased considerably, thereby adversely affecting the environment. Therefore, airlines are seeking different approaches to reduce the environmental degradation. In this paper, we study cruise speed control to achieve this goal by reducing CO_2 emissions while studying passenger service level. We use some indicators to measure the passenger service level in the airline industry. These indicators create a conflict between CO_2 emissions and passenger service level. We develop a bi-objective mixed-integer non-linear programming model to integrate flight scheduling, aircraft-path assignment, and gate assignment with the aim of reducing CO_2 emissions while increasing passenger service level. Based on a real problem, the model can lead to 11% and 31% improvement in CO_2 emissions and passenger service level, respectively. The model is NP-hard. Therefore, we develop a new constructive heuristic method, and we also use the multi-objective simulated annealing algorithm and extend this algorithm to enhance its performance. We also use the design of experiment and Taguchi method to optimize the algorithms parameters. Finally, we evaluate the proposed methods based on information retrieved from major U.S. airlines.

© 2018 Elsevier Ltd. All rights reserved.

1. Introduction

A report by the Intergovernmental Panel on Climate Change (IPCC) indicates that the entire transportation industry emits 6.7 GT CO_2 annually, of which the share of airline industry is 2%. Over the past decade, CO_2 emissions in the airline industry have grown by more than 6%. The IPCC predicted irreparable damage to the environment if sustainable policies are not adopted across the airline industry. This necessity has been leading the industry toward becoming more eco-friendly and greener. Various methods have been proposed to reduce CO_2 emissions in the airline industry. Cruise speed control is one of the newest tools offered for this purpose (Aktürk et al., 2014), which allows for adjusting the aircraft speed.

The first objective of our paper is to use cruise speed control to mitigate CO_2 emissions. The most important source of CO_2 emissions in the airline industry is the fuel consumed by aircraft. Fuel consumption accounts for about 30% of operating costs, making the fuel one of the most expensive resources in the industry (IATA, 2010). So, reducing CO_2 emissions may reduce not only the operating costs, but also the adverse effects on the environment. The second objective of our paper is to use cruise speed control to create a high passenger service level. Enhanced passenger service level will in turn increase the passenger satisfaction level (Kurtulmuşoğlu et al., 2016). We use some indicators for measuring the passenger service level, which are affected by aircraft speed. Given the inherent conflict between the two objectives, we use cruise speed control to analyze the trade-off between them.

The benefits offered by the airline industry have given an unprecedented value to it. These benefits include cost and time savings, ease of passengers transport, and high security. In 2002, the airline industry carried 1.2 million passengers worldwide, created, either directly or indirectly, 28 million jobs, and carried 40% of the merchandise trade (Barnhart et al., 2003). The industry is, however, facing challenges including air pollution control, high operational costs, and airport congestion (Díaz-Ramírez et al., 2014), thereby making the industry more complicated. As a response, the industry

* Corresponding author.
E-mail addresses: Mahdi.Jalalian@email.kntu.ac.ir (M. Jalalian), s_gholami@kntu.ac.ir (S. Gholami), Ramezanian@kntu.ac.ir (R. Ramezanian).

https://doi.org/10.1016/j.jclepro.2018.09.139
0959-6526/© 2018 Elsevier Ltd. All rights reserved.

needs planning to resolve the challenges and enjoy the advantages. Planning can be undertaken at strategic and/or operational level. Strategic planning refers to construction of airport, aircraft purchase, and flight path development. These activities are highly dependent on circumstances. Operational planning, on the other hand, refers to activities maximizing the use of resources such as flight scheduling, aircraft-path assignment, and gate assignment. The main focus of our paper is the integration of flight scheduling, aircraft-path assignment, and gate assignment with the aim of reducing CO_2 emissions while increasing passenger service level. We develop a bi-objective mixed integer non-linear programming (MINLP) model for the research problem. The main contributions of our paper are summarized as follows:

1. Developing a green model for the integration of flight scheduling, aircraft-path assignment and gate assignment;
2. Using a new objective function to examine passenger service level and some indicators for measuring it;
3. Developing a green concept for the problem; and
4. Developing a constructive heuristic algorithm, using the multi-objective simulated annealing algorithm and extending this algorithm to enhance its performance.

This paper is organized as follows. Section 2 reviews the relevant literature. Section 3 presents a new mathematical model and a numerical example for validation of the model. Section 4 provides solution methods for the model. Section 5 presents the computational results and analysis. Finally, Section 6 states concluding remarks and presents some suggestions for future research.

2. Literature review

This section reviews the earlier research related to our paper. Here are some of the approaches that have been introduced to reduce fuel consumption and CO_2 emissions. Cavcar and Cavcar (2004) analyzed the impact of aircraft performance on fuel consumption. They also analyzed climb and cruise phase of a flight. Brueckner and Zhang (2010) examined the effects of CO2 emissions charges on air fuel consumption, and found that emissions charges would raise aircraft fuel efficiency. Prats and Hansen (2011) studied allowable air delay by flying at slower speeds to reduce fuel consumption. Ryerson and Kim (2014) studied the impact of airline merges on reducing fuel consumption and passenger service level degradation. Turgut et al. (2014) explored the effects of altitude, aircraft speed and aircraft weight on fuel consumption. They noted that 1 ton reduction in aircraft mass, 1000 ft increase in flight altitude, and 1 knot decrease in cruise speed lead to 15–21 kg, 26–28 kg, and 7.7–7.8 kg less fuel consumption, respectively. Franco and Rivas (2014) observed the effects of average horizontal wind on minimum aircraft fuel consumption with a fixed altitude and arrival time. They also analyzed the aircraft weight and cruise altitude. The European Union Emission Trading Scheme (EU ETS) is a measure of CO_2 emissions reduction that should fulfill the targets specified under the Kyoto Protocol. Miyoshi (2014) measured the impact of the EU ETS on an airline to investigate equity issues as the most significant issue of the protocol. Dalmau and Prats (2015) studied continuous climb operations, which could save fuel and time by 0.5%–2% and 1%–5%, respectively. Hagmann et al. (2015) distributed self-completion questionnaires among passengers to collect data about the passengers' imaginations about green or eco-friendly airlines. They noted that passengers see the greenness as a distinctive characteristic for an airline and are willing to pay more for a greener flight. Scotti and Volta (2015) measured CO_2 emissions of the European airlines and developed an index to account for CO_2 emissions in environmental-sensitive productivity of airlines. They showed that improvements in load factor and aircraft size affect the productivity positively. Abdullah et al. (2016) introduced three benchmarks to measure green activities of airlines. These benchmarks include: (1) daily operation activities, (2), corporate environment management practices, and (3) corporate policies and strategic planning. With these benchmarks, a practical process could be implemented to improve airline sustainability. Kılkış and Kılkış (2016) developed an index for ranking airports in terms of sustainability, i.e. to benchmark performance of airports based on sustainability. The index includes energy consumption, CO_2 emissions, and service quality. Cui and Li (2016) presented a new model to study airline energy efficiency. They divided the efficiency into two categories called efficiency at operations stage and that at carbon abatement stage. Cui et al. (2016) proposed a new model and used regression method to analyze different factors affecting the energy efficiency of an airline. They introduced the average service age of fleet size and average haul distance as the most important factors influencing the energy efficiency of an airline. Li et al. (2016) measured the impact of the EU ETS on airline efficiency and considered efficiency at three stages: (1) operations stage, (2) service stage and sales stage, and (3) greenhouse gases emissions. They established two models to evaluate the efficiency. Cui and Li (2017) proposed two models based on natural and managerial disposability to analyze various impacts of "Carbon Neutral Growth from 2020 (CNG 2020)" on airline efficiency. The results revealed that CNG2020 has little influence on airline efficiency. Fukui and Miyoshi (2017) examined the impact of tax on aircraft fuel consumption and found that in the short run, an increase in the fuel tax reduces the aircraft fuel consumption.

Many studies have examined the service quality of airlines, of which the most important ones are addressed further. Suki (2014) investigated the effect of service quality on passengers' satisfaction in the Malaysia airlines. This researcher noted that there is a consistent relationship between service quality and passengers' satisfaction affected by empathy. Chow (2014) studied the service quality in Chinese airlines and examined the impact of service quality on passengers' satisfaction. This study considered passengers' complaints as the measure of the passengers' satisfaction, and on-time performance along with baggage handling service as the measure of service quality. The results indicated that passengers' satisfaction increases with service quality. Also, on-time performance has no significant impact on passengers' complaints, but low baggage handling service (such as damaged baggage) increases passengers' complaints. Vlachos and Lin (2014) examined the factors affecting service quality and passengers' loyalty. They studied Chinese airlines and divided the factors into three categories: (1) operational factors (2), competitive factors, and (3) attractive factors. They introduced aircraft, reputation, frequent flyer program, and in-flight service as the most effective factors. Hussain et al. (2015) investigated passengers' satisfaction by determining the dimensions of service quality in the Dubai airline. The results indicated that service quality has a positive significant effect on passengers' satisfaction. Jiang and Zhang (2016) studied the relationship between service quality and passengers' satisfaction in Chinese domestic airlines. They divided the passengers into two groups: business and leisure travelers. They found that the ticket price has a significant effect on passengers' satisfaction, which promotes loyalty among the leisure travelers while being insignificant for business travelers. Kurtulmuşoğlu et al. (2016) used a stochastic model to identify passengers' priorities in airline selection. They identified ticket prices, punctuality, and booking convenience as the most important priorities.

Cruise speed control is now a mature field in the operational research which is now being spun out into a new tool to control fuel consumption and CO2 emissions. This issue has been explored in

previous studies by Şafak et al. (2017), Gürkan et al. (2016), Gholami et al. (2016), Duran et al. (2015), and Aktürk et al. (2014).

What we know about the cruise speed control is largely based on these studies. All of these studies have presented a mathematical model which is non-linear because of the fuel cost function, where the cruise flight time has been considered as a decision variable. Şafak et al. (2017), Gürkan et al. (2016), Duran et al. (2015), and Aktürk et al. (2014) followed a conic program approach to reduce the problem complexity. Aktürk et al. (2014) used cruise speed control for the flights recovery optimization model. Their model involved flight scheduling and fleet assignment, and examined the trade-off between flight delays and cost of recovery. They noted that an increase in aircraft speed increases the fuel costs. Duran et al. (2015) studied flight scheduling. They considered a time windows for flights, and used a robust approach to examine the turnaround time between two flights under uncertainty. Gürkan et al. (2016) studied flight scheduling and fleet-path assignment. They proposed two heuristic algorithms for solving large-sized problems. Gholami et al. (2016) studied schedule design, aircraft assignment and maintenance routing problems. Eventually, Şafak et al. (2017) integrated flight scheduling and path assignment. They suggested two heuristic algorithms for solving the problem.

All of the above studies suggest that cruise speed control has been developed into a new area of research in recent years. One of the main issues in our knowledge about cruise speed control is a less study of gate assignment and service quality. So, we examine the gate assignment with flight scheduling and aircraft-path assignment considering cruise speed control, and develop a model for the mentioned problem with the goal of minimizing CO_2 emissions while maximizing passenger service level.

3. Problem description

Our paper reviews flight scheduling, aircraft-path assignment, and gate assignment, with Fig. 1 representing these activities. We adopted the study of Barnhart and Cohn (2004) for these activities.

The first stage involves gate assignment and flight scheduling, as these closely interact with one another. Gate assignment defines a gate for each flight. The gates are not available at any given time. Flight scheduling determines the departure and arrival times for flights. The second stage is aircraft assignment, which assigns aircraft to flights. The third stage is path assignment and attempts to assign the maximum path to one aircraft for maximizing its use during the planning horizon. Integration of the above activities is NP-hard, since the path assignment is known as NP-hard (Parmentier, 2013).

3.1. Proposed MINLP model

The reality-based model is developed with the following logical assumptions.

- The aircraft flies at a constant speed along the path, and
- The departure and arrival times of each flight occur on the same day.

Fig. 1. Flight planning procedure.

Based on the problem notation in Appendix A, the bi-objective MINLP model for minimizing CO_2 emissions and maximizing passenger service level (or minimizing the cost) is presented as follows:

$$Min \left\{ \sum_{i\in F}\sum_{t\in T}\sum_{l\in L} \tau \times c_{co_2} \times F_i(f_{it}) \times w_{itl} + \sum_{i\in F}\sum_{t\in T}\sum_{d\in D} Daily_t \times y_{itd} \right\} \tag{1}$$

$$Min \left\{ \sum_{i\in F}\sum_{t\in T} 60 \times \gamma \times f_{it} + \sum_{i\in F}\sum_{t\in T}\sum_{d\in D}\sum_{o\in G} \vartheta \times \left(wd_o^{on_i} \times g_{io}^{on_i} + wd_o^{dn_i} \times g_{io}^{dn_i} \right) \right\} \tag{2}$$

Subject to.

$$\sum_{t\in T}\sum_{d\in D} v_{itd} = 1\partial \quad \forall i\in F \tag{3}$$

$$\sum_{j\in F}\sum_{t\in T}\sum_{d\in D} x_{ijtd} \le 1 \quad \forall i\in F \tag{4}$$

$$\sum_{i\in F}\sum_{j\in F(j\neq i)} x_{ijtd} \ge \sum_{i\in F} v_{itd} - 1 \quad \forall t\in T, d\in D \tag{5}$$

$$\sum_{i\in F(i\neq j)} x_{ijtd} + \sum_{i\in F(i\neq j)} x_{jitd} \le 2 \times v_{jtd} \quad \forall j\in F, t\in T, d\in D \tag{6}$$

$$\sum_{i\in F} v_{itd} \le bigM \times e_{td} \quad \forall t\in T, d\in D \tag{7}$$

$$\sum_{i\in F} y_{itd} = e_{td} \quad \forall t\in T, d\in D \tag{8}$$

$$\sum_{i\in F} z_{itd} = e_{td} \quad \forall t\in T, d\in D \tag{9}$$

$$y_{itd} \le v_{itd} - \sum_{j\in F} x_{jitd} \quad \forall i\in F, t\in T, d\in D \tag{10}$$

$$z_{itd} \le v_{itd} - \sum_{j\in F} x_{ijtd} \quad \forall i\in F, t\in T, d\in D \tag{11}$$

$$\sum_{i\in F} v_{itd} - 1 \le (N(F) - 1) \times \sigma_{td} \quad \forall t\in T, d\in D \tag{12}$$

$$y_{itd} + z_{itd} \le 2 - \sigma_{td} \quad \forall i\in F, t\in T, d\in D \tag{13}$$

$$\sum_{j\in F} y_{jt(d+1)} = z_{itd} \quad \forall i\in F, t\in T, d\in D/d_{lt} \tag{14}$$

$$dp_i \geq \sum_{d\in D} st_d \times v_{itd} + E[NC_i] \quad \forall i\in F, t\in T \tag{15}$$

$$ar_i \leq \sum_{t\in T}\sum_{d\in D} ft_d \times v_{itd} \quad \forall i\in F \tag{16}$$

$$\sum_{l\in L} w_{itl} = \sum_{d\in D} v_{itd} \quad \forall i\in F, t\in T, l\in L \tag{17}$$

$$sp_{it}^{\min} \leq sp_{tl} \times w_{itl} \leq sp_{it}^{\max} \quad \forall i\in F, t\in T \tag{18}$$

$$f_{it} = \sum_{l\in L} \frac{ds_i}{sp_{tl}} \times w_{itl} \quad \forall i\in F, t\in T \tag{19}$$

$$ar_i = dp_i + \sum_{t\in T}\sum_{d\in D} f_{it} \times v_{itd} \quad \forall i\in F \tag{20}$$

$$dp_j \geq ar_i + TP_{ij} + E[NC_i] + E[NC_j] - bigM \times \left(1 - p_{ij}\right) \quad \forall i, j_{(i\neq j)}\in F \tag{21}$$

$$dp_j \geq ar_i + \sum_{t\in T}\sum_{d\in D} TA_{ijt} \times v_{itd} + E\left[NC_i\right] + E\left[NC_j\right] - bigM \times \left(1 - \sum_{t\in T}\sum_{d\in D} x_{ijtd}\right) \quad \forall i, j_{(i\neq j)}\in F \tag{22}$$

$$\sum_{o\in G} g_{io}^{on_i} = 1 \quad \forall i\in F \tag{23}$$

$$\sum_{o\in G} g_{io}^{dn_i} = 1 \quad \forall\, i\in F \tag{24}$$

$$\left(dp_j - ar_i\right) \times \left(dp_i - ar_j\right) \times g_{io}^{dn_i} \times g_{jo}^{on_j} \leq bigM \times \left(1 - u_{ij}\right) \quad \forall i, j\in F, o\in G \tag{25}$$

$$\left(dp_j - dp_i\right) \times \left(dp_i - dp_j\right) \times g_{io}^{on_i} \times g_{jo}^{on_j} \leq bigM \times \left(1 - mo_{ij}\right) \quad \forall i, j\in F, o\in G \tag{26}$$

$$\left(dp_j - dp_i\right) \times \left(dp_i - dp_j\right) \times g_{io}^{on_i} \times g_{jo}^{on_j} \leq bigM \times \left(1 - mo_{ij}\right) \quad \forall i, j\in F, o\in G \tag{27}$$

$$e_{td},\ v_{itd},\ w_{itl},\ x_{ijtd},\ y_{itd},\ z_{itd}, g_{io}^{on_i}, g_{io}^{dn_i} \in \{0, 1\} \quad \forall i, j\in F, t\in T, d\in D,\ l\in L,\ o\in G \tag{28}$$

$$\sigma_{td},\ f_{it},\ dp_i,\ ar_i \geq 0 \quad \forall\ i\in F,\ t\in T,\ d\in D \tag{29}$$

The objective function (1) presents green considerations. This objective reduces the environmental degradation in two different ways: (I) fuel consumption control and (II) maximal use of highly-efficient aircraft and minimal use of low-efficiency aircraft. Different equations have been proposed for calculating fuel consumption. We used the equation provided by EUROCONTROL (2012). This equation is a function of the cruise flight time, which is calculated by Equation (30).

$$F_i(F_{ti}) = \begin{cases} c_1^{i,t} \times \dfrac{1}{f_{it}} + c_2^{i,t} \times \dfrac{1}{f_{it}^2} + c_3^{i,t} \times f_{it}^3 + c_4^{i,t} \times f_{it}^2 & \text{if } v_{itd} = 1 \\ 0 & \text{if } v_{itd} = 0 \end{cases} \tag{30}$$

where $c_1^{i,t}$, $c_2^{i,t}$, $c_3^{i,t}$ and $c_4^{i,t}$ represent fuel consumption coefficients related to the aerodynamic characteristics of aircraft, air density, and gravitational acceleration of the earth. These coefficients are available in EUROCONTROL (2012) for different types of aircraft. Each kilogram of aircraft fuel consumption emits 3.15 kg of CO_2 ($\tau = 3.15$). The first term in (1) calculates CO_2 emissions costs. The second term in (1) tries to model the second approach to attenuate environmental degradation.

The objective function (2) calculates the passenger service level. The cruise flight time is an indicator of passenger service level. This topic is debatable from two viewpoints.

(I) Gronau (1970) examined the effect of the cruise flight time on passenger demands. This researcher introduced this time as an important factor for passengers' satisfaction. Passengers expect the shortest cruise flight time. Addressing this expectation can naturally enhance passengers' satisfaction. (II) Various factors contribute to a possible accident during a flight. By studying these factors, Skorupski (2015) estimated probability of occurrence of an accident during the cruise flight time as $\gamma = 1.55 \times 10^{-8}$ per hour of flight. Reducing the cruise flight time can reduce the risk of accident, i.e. flight safety should be enhanced as an effective factor in passenger service level (Hussain et al., 2015). The above viewpoints reveal the significance of cruise flight time in passenger service level. Therefore, the cruise flight time represents the first indicator of passenger service level. The first term in (2) minimizes the cost of cruise flight time to raise the passenger service level. In this paper, the walking distance represents the second indicator of passenger service level. Inadequate attention to gate assignment can increase the distance to be walked by passengers, making them dissatisfied. With proper gate assignment, however, this threat can be turned into an opportunity to attain passengers' satisfaction. The second term in (2) minimizes passenger walking distance to augment their service level.

Constraint (3) ensures that each flight is performed by one aircraft and within one day of planning horizon. Constraints (4)–(6) plan some flights consecutively by one aircraft. These flights are members of a set where the destination of one flight is the origin of another. The planning horizon in the proposed model is multi-day, leading to Constraints (7)–(13). Therefore, it is necessary to identify the first and last flights of aircraft in each day. Constraints (7), (8) and (10) find the first flight performed by each aircraft on each day, while Constraints (7), (9) and (11) find the last flight performed by each aircraft on each day. Constraint (12) calculates σ_{td}. If aircraft t performs only one flight on day d, then Constraint (13) considers this flight as both the first and last flight for aircraft t on day d. If,

Table 1
Published schedule.

Tail	Flight number	origin	destination	Departure time	Arrival time	Cruise flight time
N3ELA	2057	ORD	SJU	08:30	13:00	270
	2078	SJU	ORD	14:25	19:40	315
N3DUAA	2099	ORD	LAX	07:00	11:10	250
	1972	LAX	ORD	12:40	16:25	225
	1972	ORD	RDU	17:45	19:20	95
N412AA	2345	ORD	DFW	17:15	19:30	135
	2374	DFW	ORD	20:40	22:30	110
N4XGAA	2079	ORD	SAN	08:45	12:55	250
	1438	SAN	ORD	14:00	17:50	230
	346	ORD	LGA	19:50	21:45	115

however, aircraft t performs more than one flight on the day d, then Constraint (13) does not consider any of these flights as both the first and last flight for aircraft t on day d. Constraint (14) is required to know the first and last flights of all aircraft in each day. This constraint ensures that the last destination of aircraft t on a day is the same as the first origin of aircraft t on the next day. There is a curfew time in some airports due to the security issues and military regulations (Hu et al., 2016). Accordingly, Constraints (15) and (16) present the time limit for flights. According to the assumptions, Constraint (17) selects one speed level for each aircraft along the path. Given that flight speed is not an arbitrary parameter but rather depends on the path type and the fuel tank capacity, Constraint (18) controls the speed along the flight path. Constraint (19) calculates the cruise flight time. Constraint (20) shows the relationship between the departure and arrival times of one flight. If two flights have passengers in common, then Constraint (21) ensures that the departure time of the proceeding flight is later than the arrival time of the preceding flight. If two flights are performed by one aircraft, then Constraint (22) ensures that the departure time of the proceeding flight is later than the arrival time of the preceding flight. Constraints (23) and (24) assign one gate to each flight at the origin and destination airports. Considering two flights performed by two different aircraft with the origin of one flight being the destination of the other, Constraint (25) avoids simultaneous assignment of these flights to the same gate. Considering two flights with the same origin, Constraint (26) avoids simultaneous assignment of these flights to the same gate. Considering two flights with the same destination, Constraint (27) avoids simultaneous assignment of these flights to the same gate. Constraints (28) and (29) represent binary and non-negative variables, respectively.

3.2. Uncertainty in the parameters

We divided the time into two parts: (I) cruise flight time, i.e. the time between take-off and landing of the aircraft, and (II) non-cruise time, i.e. the time related to taxi-in, taxi-out, as well as climbing and descending stages. The non-cruise time is uncertain in the environment. Similar to the study of Şafak et al. (2017), we used the expected value to address the associated uncertainty with this time. Equation (31) calculates the non-cruise time.

$$E[NC_i] = \frac{e^{\alpha}}{(1-\beta_i)\times(1+\beta_i)} \quad \forall i \in F \tag{31}$$

where e^{α} is 15, so non-cruise time can deviate from its mean value by up to 15 min. Also, β_i is defined to estimate the airport congestion, as calculated in Equation (32).

$$\beta_i = \beta \times (e_{on_i})^2 \times (e_{dn_i})^2 \quad \forall i \in F \tag{32}$$

where β is a constant, and e_{on_i} and e_{n_i} explain the congestion coefficient for the origin and destination airports of flight i, respectively. Şafak et al. (2017) provided the value of these coefficients. Consideration of airport congestion makes the non-cruise time closer to the actual value. Further, airport congestion affects the turnaround time and the turntime, as calculated in Equations (33) and (34).

$$Tp_{ij} = \delta \times e_{dn_i} (= e_{on_j}) \quad \forall i,j \in F \tag{33}$$

$$TA_{ijt} = \eta \times e_{dn_i} (= e_{on_j}) \quad \forall i,j \in F, t \in T \tag{34}$$

where δ and η are constants.

3.3. Numerical example

This section provides a numerical example (called published schedule) to study the efficiency of the model. Table 1 describes the published schedule.

Each tail includes different flights performed by one aircraft. There are differences between the published schedule and proposed schedule in our paper. These differences are due to the consideration of CO_2 emissions and passenger service level. These two objectives are conflicting in nature.

3.3.1. Conflicting objectives

Applying the model for the flights listed in Table 1 led to five Pareto solutions, as shown in Fig. 2. We examined the model using the augmented ε-constraint (Aug.eps) method.

Optimal CO_2 emissions and passenger service level costs are observed in two different Pareto solutions, suggesting that these objectives cannot be optimized simultaneously. Each Pareto solution has a different schedule. In Pareto1, CO_2 emissions costs are maximal since all flights were set to be performed at the fastest speed levels. The proposed schedule in Pareto 1 is not economical in terms of green considerations, but gives the best passenger service level by minimizing the cruise flight time. So, passenger service level is maximal and its cost is minimal. As we proceed to Pareto 5, CO_2 emissions decrease since flights were set to be performed at lower speed levels. Pareto 5 is ideal in terms of green considerations, but gives the worst passenger service level by maximizing the cruise flight time. So, passenger service level is minimal and its cost is maximal.

3.3.2. Proposed schedule by the model

The published schedule used four aircraft, with Fig. 3(a) representing this schedule. Gürkan et al. (2016) tested their model using

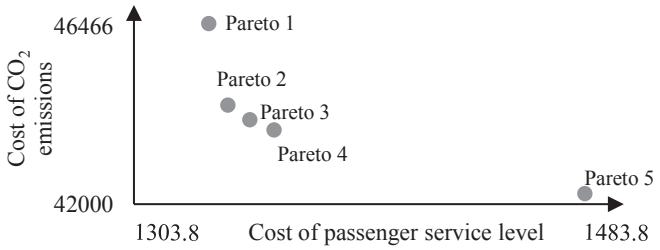

Fig. 2. The proposed schedule by the model.

the published schedule. According to the information in their study, aircraft efficiency is different. Gürkan et al. (2016) managed to schedule all flights with three aircraft. Indeed, their model omitted the most expensive aircraft. Fig. 3(b) shows the schedule presented by Gürkan et al. (2016). Our proposed model provided an entirely different schedule compared with the two above schedules. Our proposed model used only two aircraft across all Pareto solutions. Similar to Gürkan et al. (2016) study, our proposed model omitted the most expensive and inefficient aircraft from the schedules of all Pareto solutions. Also, the model used the most efficient aircraft in the schedules of all Pareto solutions. Table 2 compares the costs of the three above schedules.

Reducing the number of aircraft reduces the daily cost of their usage. Gürkan et al. (2016) improved this cost by about 26% compared with the published schedule. On average across all Pareto solutions, our proposed model improved this cost by about 49% compared with the published schedule.

Gürkan et al. (2016) improved CO_2 emissions costs by about 10% compared with the published schedule. Our proposed model improved CO_2 emissions costs by about 6.37% and 15% for the worst (Pareto 1) and the best case (Pareto 5), respectively, compared with the published schedule. Such improvements were obtained upon speed control and aircraft assignment.

The cost of passenger service level was calculated for the schedule presented by Gürkan et al. (2016), where the cost was improved by about 2.7% compared with the published schedule. Our proposed model improved the cost of passenger service level by about 25% and 33% for the worst (Pareto 5) and the best case (Pareto 1), respectively, compared with the published schedule.

The choice of Pareto solution depends on the airline policies. For instance, restrictions on CO_2 emissions and passenger flow affect such decision. There are several approaches to help decision-makers choose one Pareto solution. In this paper, TOPSIS (Technique for Order of Preference by Similarity to Ideal Solution) was adopted for this purpose. We refer readers to Hwang and Yoon (1981) for more information on this technique. TOPSIS found Pareto 4 in Fig. 2. Table 3 and Fig. 3(c) represent the schedule for this Pareto solution. In our opinion, the results confirm the validity of the model proposed in this paper.

In Fig. 3, each color represents a tail. The horizontal lines represent the turnaround time, the turntime and the non-cruise time, while diagonal lines represent the cruise flight time.

4. Solution methods

We use the Aug.eps method to solve the bi-objective MINLP model. This method is used to obtain Pareto optimal solutions. The readers can refer to Mavrotas (2009) for more information on the method. The model is NP-hard, so application of such techniques as the Aug.eps method to solve the problem is time consuming. This section provides some heuristic and meta-heuristic algorithms which can potentially solve the problem within a short time.

4.1. Constructive heuristic algorithm based on speed level

The heuristic algorithm is called constructive heuristic algorithm based on speed level (CHSL). Steps of the heuristic are presented herein. In the first step, all aircraft are set at their highest speed, thereby making f_{it} a parameter. In the second step, the model is solved based on the adjusted speed. In this situation, CO_2 emissions are maximal, but it offers the best passenger service level. In the third step, the aircraft with the highest CO_2 emissions is selected and its speed is reduced by one level, thereby reducing CO_2 emissions. Then, f_{it} is updated and the second step is repeated. The heuristic continues until the speed of all aircraft is minimized. In this case, CO_2 emissions are minimal, but it offers the worst passenger service level. Each time, the second step obtains one Pareto solution. Heuristic 1 demonstrates the CHSL.

Heuristic 1
Constructive Heuristic algorithm based on Speed level (CHSL).

Input: Parameters introduced in section 3.1
Begin
Step 0. (initialization)
Set counter $itr = 0$;
Set $neff = \{\}$;
Step 1. (initial speed)
Set the speed of aircrafts at maximum level;
Solve the bi-objective MINLP model based on the adjusted speed;
let P_{itr} denotes the obtained Pareto solution at iteration itr;
$neff = P_{irt} \cup neff$;
Let sp_{n_min} denotes the set of aircrafts that their speed are not at minimum level;
Step 2. (decreasing speed)
While $sp_{n_min} \neq \{\}$ **do**
Choose an aircraft with maximum CO_2 emissions;
Let t_{itr} denotes the chosen aircraft at iteration itr;
Decrease the speed of aircraft t_{itr} by one level;
update sp_{n_min};
Solve the bi-objective MINLP model based on the update speed;
let P_{itr} denotes the Pareto solution;
$itr = itr + 1$;
$neff = P_{irt} \cup neff$;
End
Step3.
Apply non-dominated solution selection algorithm on set $neff$;
End
Output: Set of non-dominated Pareto solutions (neff)

4.2. Multi-objective simulated annealing

We use the multi-objective simulated annealing algorithm (MOSA) and extend it to enhance its performance. The solution representation, initial solution generation, and neighborhood generation are described in the following. Finally, the pseudo code of the extended MOSA is presented. Fig. 4 shows the solution representation of the problem.

Each solution contains a matrix called ∅. n and r denote the row

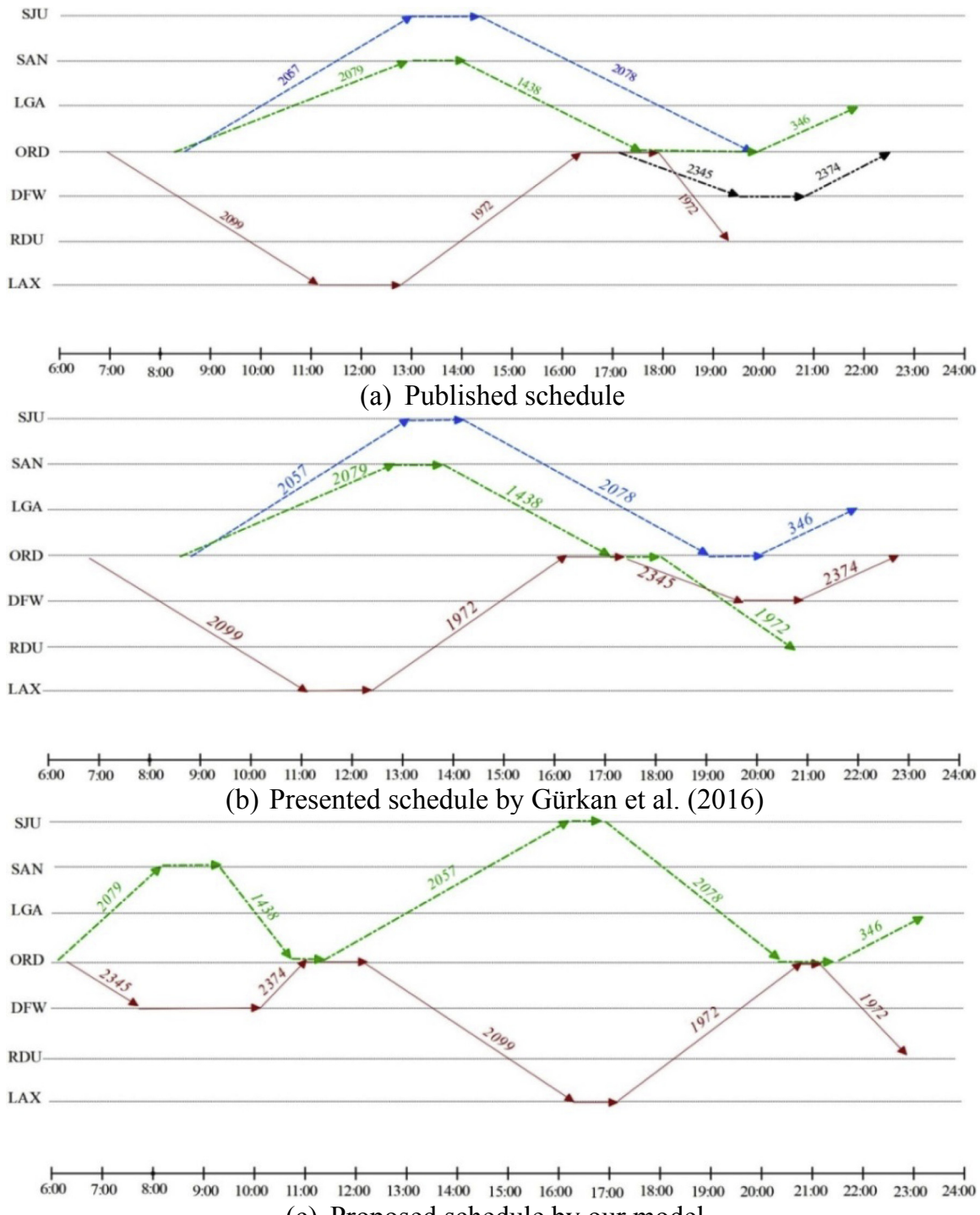

Fig. 3. Comparison among different schedules.

Table 2
Cost comparison.

Schedule	Proposed schedule by our model					Published schedule	Gürkan et al., 2016
Cost	1	2	3	4	5		
Daily usage	171,600	176,400	171,600	176,400	176,400	345,600	255,600
CO2 emissions	46,526	44,485	44,105	43,860	42,260	49,696.8	44,485
Passenger service level	1333.8	1341.5	1345.3	1349.5	1484.4	1995	1941.8

and column numbers, respectively. Odd rows include flight number and even rows include aircraft speed for the flight in the previous row, respectively. The odd row number indicates the aircraft number, where: $t = \frac{n+1}{2}\ \forall n = 1, 3, \ldots$. The set of flights in an odd row form the aircraft path. The column number represents the position of the flight in the path. Accordingly, the number zero corresponds to the flights that do not exist in reality. If no flights are assigned to an aircraft, then the values along all columns corresponding to that aircraft will be zero (like aircraft 3 in row 5). Fig. 4 shows aircraft-path assignment. The stated problem involves flight scheduling and gate assignment as shown in Algorithm 1 and Algorithm 2, respectively.

Algorithm 2 presents the pseudo code followed to generate the initial solution including gate assignment. This algorithm adopts the roulette wheel algorithm to assign gates. Each gate has a weight based on its distance to entrance/exit, whereby the probability of choosing the gates with the shortest distance increases.

Five methods are used for neighborhood generation: (1) altering aircraft assignment, (2) altering gate assignment, (3) altering aircraft speed, (4) breaking path: one path is broken down into two paths and an unused aircraft is assigned to the new path, and (5) path connection: if two paths (performed by two different aircraft) have common origin or destination, then they will be merged into one path and performed by one aircraft.

Input: $\phi, N(F), N(T), E[NC_i], st_d, ds_i, TA_{ge}, TP_g$

Begin

Step 0. (initialization)

Set counter n =1;

Set counter r =1;

Step 1.

While $n \le 2N(T) - 1$ **do**

  If $\phi(n,r) = 0$ **then**

    n=n+2;

  Else

$$dp_{\phi(n,r)} = st_{d=1} + E[NC_{\phi(n,r)}]; \qquad \forall n = 1,3,5,\ldots,2N(T)-1,\ \forall r = 1 \tag{35}$$

$$dp_{\phi(n,r)} = \max\left\{ar_{\phi(n,r-1)} + TA_{\phi(n,r-1),\phi(n,r),\frac{n+1}{2}} + E[NC_{\phi(n,r-1)}] + E[NC_{\phi(n,r)}],\ ar_{\phi(n,r-1)} + TP_{\phi(n,r-1),\phi(n,r)} + E[NC_{\phi(n,r-1)}] + E[NC_{\phi(n,r)}]\right\}; \qquad \forall n = 1,3,\ldots,2N(T)-1,\ \forall r = 2,,3,\ldots,N(F) \tag{36}$$

$$ar_{\phi(n,r)} = dp_{\phi(n,r)} + \frac{ds_{\phi(n,r)}}{\phi(n+1,r)}; \qquad \forall n = 1,3,5,\ldots,2N(t)-1,\ \forall r = 1,2,3,\ldots,N(F) \tag{37}$$

    End

    If $r \ge N(F)$ **then**

      r=1;

      n=n+2;

    Else

      r=r+1;

    End

  End

End

End

Output: Flight scheduling

Algorithm 1. Flight scheduling.

Input: *G,T,F,L*
Begin
Step 0. (initialization)
F= {1, 2, …};
T= {1, 2, …};
Let u_i represents the set of flights whose origin is the destination of flight i;
Let $\emptyset$ represents the matrix including the flights, aircrafts and speed levels (Fig. 4,);
$\emptyset = \{\}$;
Step 1. (assign path to aircraft)
  While $F \neq \{\}$ **do**
    Choose aircraft t ($t \in T$) randomly ;
    Remove aircraft t from T ;
    Choose flight i ($i \in F$) randomly ;
    Remove flight i from F ;
    Assign flight i to aircraft t ;
    Choose one speed level l ($l \in L$) for aircraft t in flight i randomly;
    Assign gate o ($o \in G$) to flight i based on the roulette wheel;
    r=1;
    n=2t-1;
    $\emptyset(n,r) = i$;
    While u_i={} **do**
      Choose flight j ($j \in u_i$) randomly ;
      Remove flight j from F;
      Choose speed level l ($l \in L$) for aircraft t in flight j randomly;
      Assign gate o ($o \in G$) to flight j based on the roulette wheel;
      r=r+1;
      $\emptyset(n,r) = j$;
      i=j;
    End
    If $F \neq \{\}$ & T={} **then**
      Infeasible solution is obtained, so step 0 is run again;
      Break the loop;
    End
  End
Step 2. (determine flight schedule)
Apply Algorithm 1 to schedule the flights;
Step 3. (Gate simultaneous assignment)
While there is a Gate simultaneous assignment **do**
  Let *G_Sim* denotes the set of flights which caused a gate simultaneous assignment;
  Choose flight i ($i \in G_Sim$) randomly;
  Remove gate o that has been assigned to flight i;
  Perform roulette wheel without considering gate o;
  Assign new gate to flight i;
End
End

Output: Initial solution includes aircraft-path assignment (matrix $\emptyset$), flight scheduling and gate assignment

Algorithm 2. Initial solution.

4.2.1. Modified population-based metaheuristic for multi-objective simulated annealing

In each step of the MOSA, only one solution and one neighborhood are generated. The readers can refer to Engrand (1998) for detailed description of this algorithm. There exist many methods for increasing the search space of the MOSA, with using population being one of these methods. In this case, several initial solutions are considered and several neighborhoods are generated for each of them. We extended a part of the MOSA based on the multi-objective particle swarm optimization (step 2 in Algorithm 3) called modified population-based metaheuristic for multi-objective simulated annealing (MPMSA). Algorithm 3 presents the pseudo code of the MPMSA.

Input: population size (*pop*), number of neighborhood (*move*), initial temperature (T_0), minimum temperature (T_{min}), cooling rate (α), number of iterations (*sub_itr*)

Begin

Step 0. (initialization)

P_solution={};

Let *max_sub_itr* denotes the last counter of *sub_itr* ;

Tem= T_0 ;

for *sub_itr* =1: *max_sub_itr*

ND={};

Step 1. (generate populations and neighborhoods)

Generate *pop* feasible solutions based on Algorithm 2;

Let *pop*(*p*) denotes the *p*-th solution;

Save the *pop* solutions in *ND*;

While *Tem*> T_{min} **do**

for *p*=1:*pop* **do**

for *q*=1:*move* **do**

ngh_pop(*p*,*q*) = generate neighborhood for *pop*(*p*);

End

End

Step 2. (sort the neighborhoods)

Let *newpop* denotes the set of all generated neighborhood solutions ($ngh_pop(p,q) \in newpop$);

Apply non-dominated solution selection algorithm on *newpop*;

Let *ndm_newpop* denotes non-dominated solutions of *newpop*;

Let *nondm_newpop* denotes the number of non-dominated solutions of *ndm_newpop*;

If *nondm_newpop* > *pop* **do**

Select *pop* solutions from *ndm_newpop*;

The selection priority is the solutions in *ndm_newpop* that have the largest Euclidean distance from other solutions (This priority will expand the search space);

Let *NEG* denotes the *pop* selected solutions;

End

If *nondm_newpop* < *pop* **do**

Select all non-dominated solutions from *ndm_newpop*;

Select *pop* - *nondm_newpop* solutions from dominated solutions of *newpop*;

The selection priority is the dominated solutions in *newpop* that have the largest Euclidean distance from other solutions;

Let *NEG* denotes the *pop* selected solutions;

End

If *nondmt_move* = *pop* **do**

Let *NEG* denotes the set of all non-dominated solutions in *ndm_newpop*;

End

for *p*=1:*pop* **do**

Choose solution *y* ($y \in NEG$) randomly;

Remove *y* from *NEG*;

If *NEG(y)* dominates *pop*(*p*) **do**

NEG(y) replaces *pop*(*p*) in set *ND*;

End

If *pop*(*p*) dominates *NEG(y)* **do**

Let f_1 denotes objective function (1) and f_2 denotes objective function (2);

$$Possibility = \exp\left(-\frac{1}{Tem}\times\left(\ln\left[\frac{f_1(NEG(y))}{f_1(pop(p))}\right]+\ln\left[\frac{f_2(NEG(y))}{f_2(pop(p))}\right]\right)\right) \quad (38)$$

Let *rnd* denotes a random number;

If *rnd* $\geq$ *possibility* **do**

NEG(y) replaces *pop*(*p*) in set *ND*;

End

End

End

P_solution = *P_solution* $\cup$ *ND*;

Tem=(1- α)%×*Tem*;

End

End

Step 3.

Apply non-dominated solution selection algorithm on *P_solution*;

End

Output: Set of non-dominated Pareto solutions *P_solution*

Algorithm 3. Modified population-based metaheuristic for multi-objective simulated annealing (MPMSA).

Table 3
The schedule proposed by the model.

Tail	Flight number	origin	destination	Departure time	Arrival time	Cruise flight time
N4XGAA	2079	ORD	SAN	06:11	08:11	120
	1438	SAN	ORD	08:45	10:45	120
	2057	ORD	SJU	11:09	16:17	308
	2078	SJU	ORD	16:57	20:50	233
	346	ORD	LGA	21:30	23:18	108
N412AA	2345	ORD	DFW	06:17	07:37	80
	2374	DFW	ORD	10:00	11:10	70
	2099	ORD	LAX	12:03	16:23	260
	1972	LAX	ORD	17:05	20:25	200
	1972	ORD	DFW	21:08	22:44	96

	$r=1$	$r=2$	$r=3$	$r=4$	$r=5$	$r=6$	$r=7$	…
$n=1$	6	7	8	9	10	0	0	…
$n=2$	900	1050	850	800	1100	0	0	…
$n=3$	1	2	3	4	5	0	0	…
$n=4$	1210	1100	950	900	1200	0	0	…
$n=5$	0	0	0	0	0	0	0	…
$n=6$	0	0	0	0	0	0	0	…

Fig. 4. Solution representation (matrix ⌀).

5. Computational results

We tested the model and solution methods based on the data collected from the major U.S. airlines. This information was collected by the Bureau of Transportation Statistics (BTS) of the U.S. Department of Transportation and retrieved at http://www.bts.gov. The Aug.eps method was coded in GAMS V.24.1.3. We considered 10 grid points for this method. The proposed CHSL method was coded in GAMS V.24.1.3 and Matlab R2015a. The metaheuristic algorithms were coded in Matlab R2015a. All the work on the computer was conducted using a PC equipped with 8 GB of RAM and an Intel Core™ i7 CPU operating by Microsoft Windows 10 (64-bit). The problems were divided into two categories: small-sized and large-sized. The combinations of small-sized and large-sized problems were $d=\{1,2\}\times t=\{5,7\}\times i=\{15,25\}$ and $d=\{2,3\}\times t=\{20,40\}\times i=\{100,300\}$, respectively.

5.1. Performance measures

Various measures are needed to evaluate solution methods for bi-objective problems. For this purpose, we used five measures as summarized in Table 4.

In Equation (39), d_i is the Euclidean distance between Solution i and its closest solution. In Equation (40), f_k^{best} denotes the ideal solution (minimum value) of the objective function k ($k=1, 2$), and f_{ki} shows the value of the objective function k for the Pareto solution i, and also $f_{k,total}^{max}$ and $f_{k,total}^{min}$ represent the maximum and minimum values of the objective function k among all Pareto solutions obtained by different methods.

5.2. Parameter setting

The MPMSA has six parameters including *pop*, *move*, T_0, $T_{\min}$, α and *sub_itr*. Design of experiment was used to determine the initial level of T_0. Temperature is a factor required for accepting dominated Pareto solutions. Accepting the dominated Pareto solutions extends the search space. Different values of T_0 in the interval [0,100] were used to calculate the probability of accepting the dominated Pareto solutions. We removed other parameters from the experiments for eliminating their effects. Therefore, each experiment was performed at T_0 without temperature reduction. In each experiment, *Sub_it* was 500. If the dominated Pareto solution replaced the current solution, then the probability of accepting the dominated Pareto solution was recorded. In each experiment, the probability of accepting the dominated Pareto solution on *Sub_it* was averaged. Each experiment was performed five times, with

Table 4
Performance measures.

Measure	explanation	Formula
Number of non-dominated Pareto solutions (CRD)	• Larger value is better	–
solving time (*CPU time*)	• Smaller value is better	–
Spacing metric (SM)	• Smaller value is better • Showing the evenly distribution of Pareto solutions along the Pareto front	$SM=\frac{\sum_{i=1}^{CRD-1}\left\lvert\overline{d}-d_i\right\rvert}{(CRD-1)\overline{d}},\ \overline{d}=\frac{1}{CRD}\sum_{i=1}^{CRD}d_i$ (39)
Mean ideal distance (MID)	• Smaller value is better • Showing the mean distance of the Pareto solutions from the ideal solution	$MID=\sum_{i=1}^{CRD}\sqrt{\frac{\left(\frac{f_{1i}-f_1^{best}}{f_{1,toral}^{\max}-f_{1,toral}^{\min}}\right)^2+\left(\frac{f_{2i}-f_2^{best}}{f_{2,toral}^{\max}-f_{2,toral}^{\min}}\right)^2}{CRD}}$ (40)
Quality metric (QM)	• Larger value is better • Showing the contribution of each method from all non-dominated Pareto solutions	$QM=\frac{Number\ of\ non-dominated\ Pareto\ solutions\ of\ the\ method}{Number\ of\ all\ Pareto\ solutions\ of\ all\ methods}$ (41)

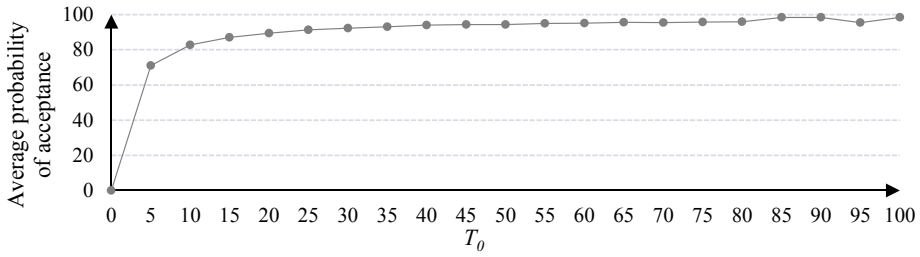

Fig. 5. The average probability of accepting the dominated Pareto solutions in T_0.

Table 5
Initial levels of the parameters in the MPMSA.

Parameter	Level	Value	Parameter	Level	Value
T_0	1	85	*Sub_it*	1	50
	2	90		2	100
	3	100		3	150
pop	1	30	*move*	1	3
	2	50		2	6
	3	70		3	9
α	1	0.5	$T_{\min}$	1	0.005×10^{-5}
	2	0.6			
	3	0.7			
	4	0.8			
	5	0.9			
	6	0.95			

Fig. 5 representing the average values.

According to the results, T_0 with values of 85, 90 and 100 obtained the highest possibility of accepting the dominated Pareto solutions. Accordingly, these values were considered as initial levels for T_0. Meanwhile, a small value was selected for $T_{\min}$. The initial levels of other parameters were determined by trial and error. Table 5 reports the results.

Taguchi method was used to determine the optimal values of the above parameters. Based on Table 5, this method proposed 18 experiments. Taguchi method was implemented by Minitab 17. Each experiment presented different Pareto solutions. In each experiment of the Taguchi method, we aggregated the values of the performance measures based on their weights to obtain a unique output. Further, Analytical hierarchy process (AHP) was used to weigh the performance measures based on their importance. Accordingly, the values of the weights were found to be $QM = MID = SM = 0.29$, $CRD = CPU\ time = 0.06$. Each experiment of Taguchi method was performed five times. Fig. 6 reports the average values as signal-to-noise (S/N) ratio.

The optimal values of the MPMSA parameters are as follows: $\alpha = 0.7$, $T_0 = 90$, $Sub_it = 100$, $pop = 30$ and $move = 3$. We applied the mentioned conditions to determine the parameters of the MOSA. The optimal values of the MOSA parameters are as follows: $\alpha = 0.5$, $T_0 = 100$ and $Sub_it = 500$.

5.3. Small-sized problems

Small-sized problems were solved by the proposed solution methods. Each problem was solved 5 times, with Table 6 and Fig. 7 reporting the average values.

Table 6 and Fig. 7 present the performance of the solution methods in small-sized problems. Statistical analyses were conducted using the IBM SPSS Statistics 22 applying a significance level of 0.05. The Kolmogorov-Smirnov test revealed that except for *QM* in the MOSA, all of the performance measures are normally distributed. We used *t*-test for normal distribution. The obtained value of *CRD* revealed that the MPMSA achieves a statistically significant improvement compared with other methods. In addition, *t*-test for the *CRD* found a statistically significant difference between

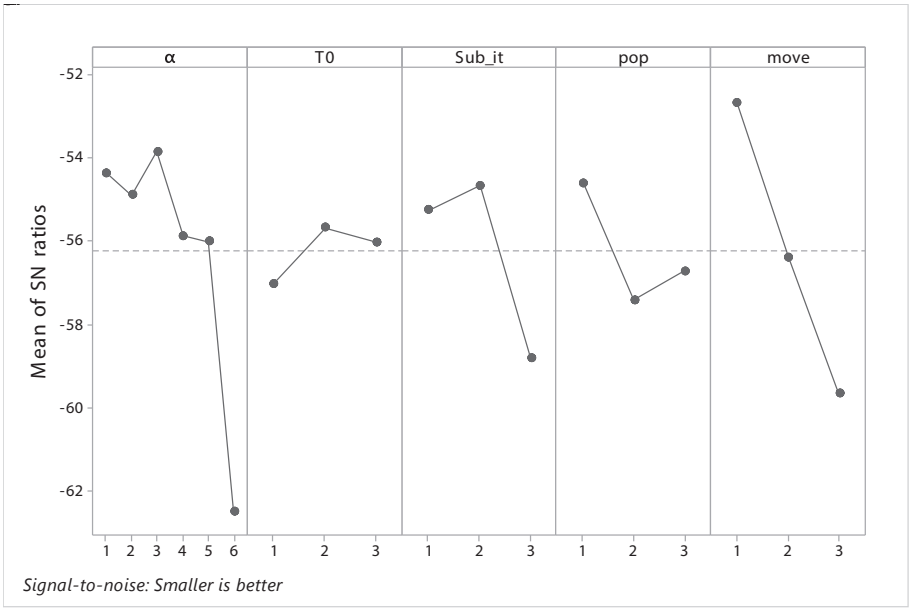

Fig. 6. S/N chart for setting the MPMSA parameters.

Table 6
Results of the performance measures in small-sized problems.

$d \times t \times i$	Aug.eps				CHSL				MOSA				MPMSA			
	CRD	SM	MID	QM	CRD	SM	MID	QM	CRD	SM	MID	QM	CRD	SM	MID	QM
$1 \times 5 \times 15$	6	0.52	0.01	0.30	6	0.30	0.01	0.15	5	0.72	0.04	0	10	0.45	0.01	0.15
$2 \times 5 \times 15$	8	1.30	0.02	0.35	9	1.72	0.02	0.33	8	0.52	0.03	0.05	13	0.50	0.02	0.20
$1 \times 7 \times 15$	4	0.50	0	0.45	8	0.33	0.03	0.25	3	1.16	0.06	0	22	1.10	0.03	0
$2 \times 7 \times 15$	9	0	0.02	0.34	11	0.33	0.02	0.24	8	0.59	0.02	0.02	28	1.01	0.02	0.10
$1 \times 5 \times 25$	7	0.67	0.01	0.43	7	0.88	0.02	0.16	6	0.89	0.05	0	13	0.67	0.03	0.16
$2 \times 5 \times 25$	6	0.62	0.01	0.60	7	0.42	0.02	0.44	4	0.76	0.09	0	18	1.05	0.04	0.11
$1 \times 7 \times 25$	5	0.36	0.01	0.38	6	0.49	0.01	0.27	6	0.80	0.02	0	15	0.68	0.02	0
$2 \times 7 \times 25$	6	1.28	0.01	0.43	7	1.34	0.01	0.29	4	2.27	0.03	0	14	0.97	0.01	0.08

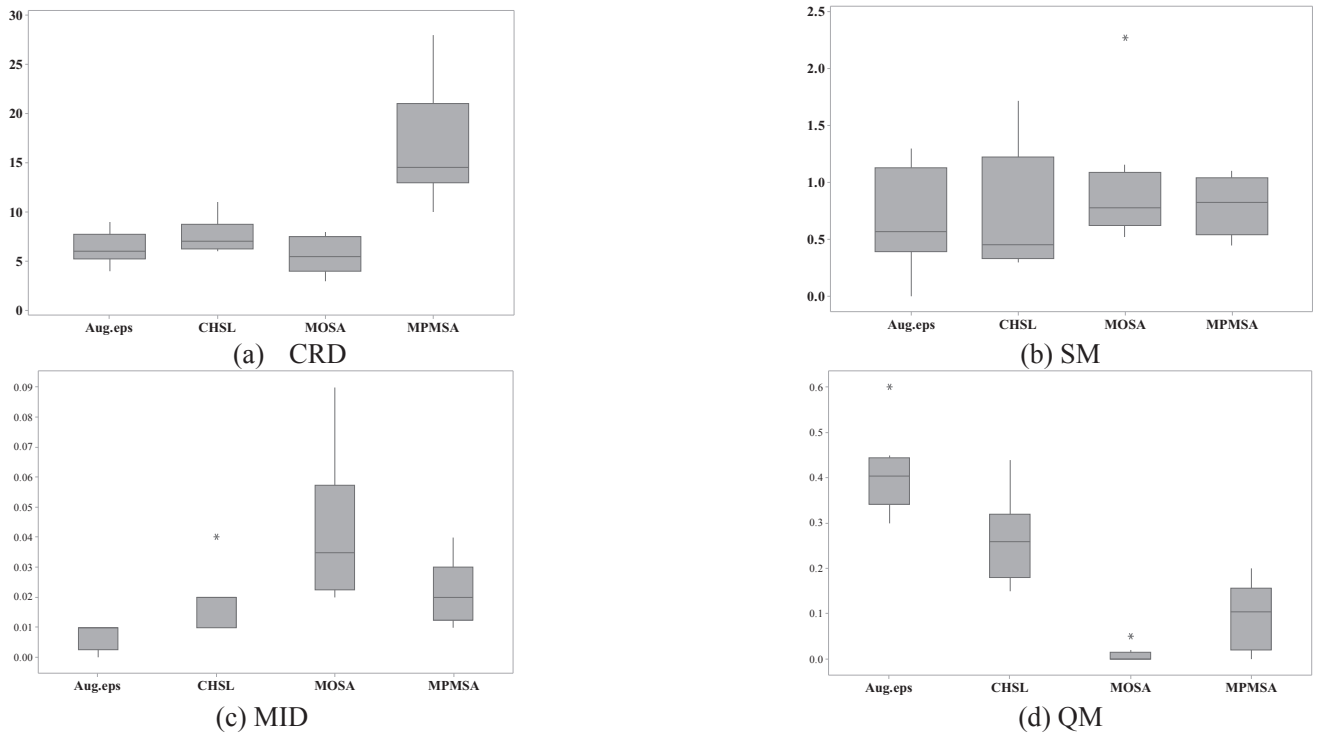

Fig. 7. Box plots of the performance measures in small-sized problems.

the CHSL and the MOSA, but found no significant differences in the remaining comparisons. The obtained value of *SM* revealed that the CHSL outperforms other methods. In addition, *t*-test for the *SM* found no significant differences among all the methods. The obtained value of *MID* revealed that the Aug.eps and the CHSL exhibit the best performance. In addition, *t*-test for the *MID* found no significant differences between the Aug.eps and the CHSL as well as between the CHSL and the MPMSA. *t*-test for the *MID* found significant differences in the remaining comparisons. The obtained value of *QM* revealed that the Aug.eps and the CHSL outperform other methods. In addition, statistical tests for the *QM* found significant differences among all the methods. Fig. 8 illustrates the *CPU time* for all methods in small-sized problems.

The problem is NP-hard, so expectedly it grows more complex upon increasing the problem size. Analysis of variance (ANOVA) was performed on the *CPU time* to discover the effect of size on this parameter. This analysis was carried out using IBM SPSS Statistics 22. According to the results, the number of flights was the only parameter exhibiting statistically significant correlation with *CPU time* in small-sized problems. Also, Fig. 8 confirms that the Aug.eps

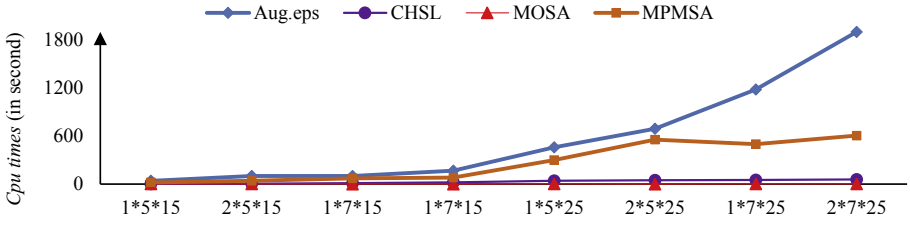

Fig. 8. *CPU time* in small-sized problems.

Table 7
Results of the performance measures in large-sized problems.

$d \times t \times i$	CHSL				MOSA				MPMSA			
	CRD	SM	MID	QM	CRD	SM	MID	QM	CRD	SM	MID	QM
$2 \times 20 \times 100$	7	0.61	0.01	0.24	4	2.54	0.04	0	27	0.65	0.01	0.16
$3 \times 20 \times 100$	9	0.61	0	0.58	2	2.25	0.04	0	29	0.64	0.03	0.15
$2 \times 25 \times 100$	8	1	0.01	0.13	3	4.38	0.03	0	35	0.83	0.01	0.08
$3 \times 25 \times 100$	7	0.83	0.01	0.35	4	4.37	0.02	0	41	1.01	0.01	0.16
$2 \times 40 \times 300$	10	0.92	0.03	0.28	5	3.98	0.06	0	34	0.80	0.03	0.10
$3 \times 40 \times 300$	10	0.88	0	0.42	5	3.52	0.05	0	45	0.88	0	0.13
$2 \times 50 \times 300$	5	0.46	0	0.39	2	1.35	0.04	0	49	0.91	0.02	0.05
$3 \times 50 \times 300$	8	0.48	0	0.34	4	6.15	0.03	0	47	0.60	0.01	0.05

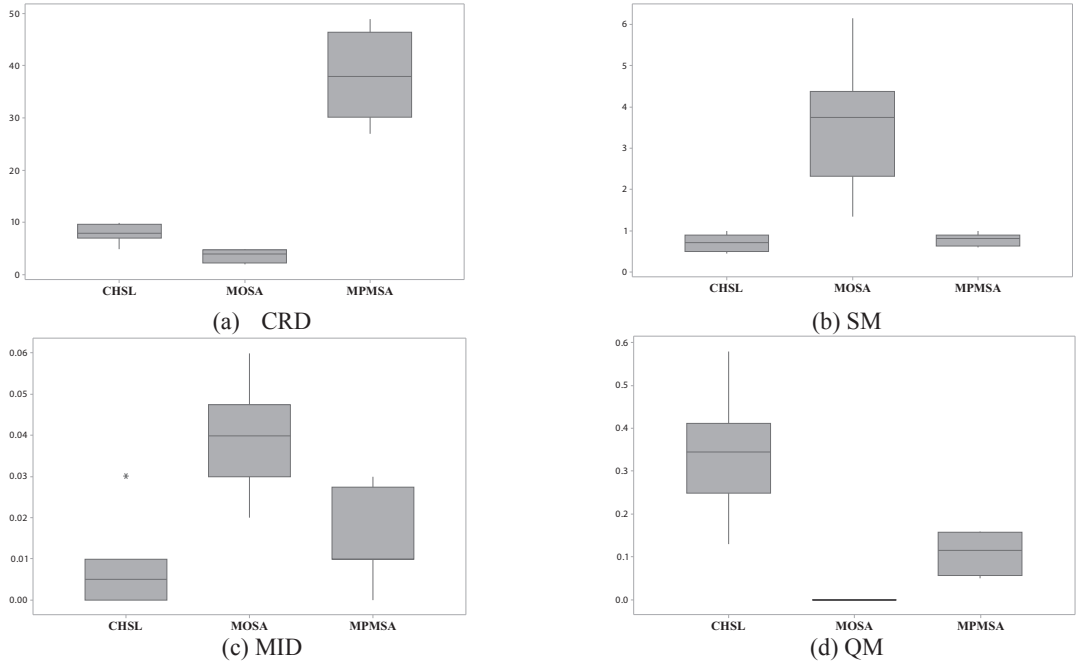

Fig. 9. Box plots of the performance measures in large-sized problems.

in terms of the *CPU time* indicates the highest sensitivity to the problem size than other methods.

5.4. Large-sized problems

Setting a time limit of 15,000 s for solving the large-sized problems, all solution methods, expect for the Aug.eps, were able to find solutions within this time. Each problem was performed 5 times, with Table 7 and Fig. 9 representing the average values.

Table 7 and Fig. 9 present the performance of the solution methods in large-sized problems. The Kolmogorov-Smirnov test revealed that except for *QM* in the MOSA and *MID* in the MPMSA, all of the measures are normally distributed. The obtained value of *CRD* revealed that the MPMSA outperforms other methods. In addition, the statistical test for the *CRD* found significant differences among all the methods. The obtained values of *SM* and the *MID* revealed that CHSL outperforms other methods. On the other hand, the statistical test for the *SM* and the *MID* found no significant difference between the CHSL and the MPMSA, but found significant differences in the remaining comparisons. The obtained value of *QM* revealed that the CHSL achieves a statistically significant improvement compared with other methods. Fig. 10 illustrates the

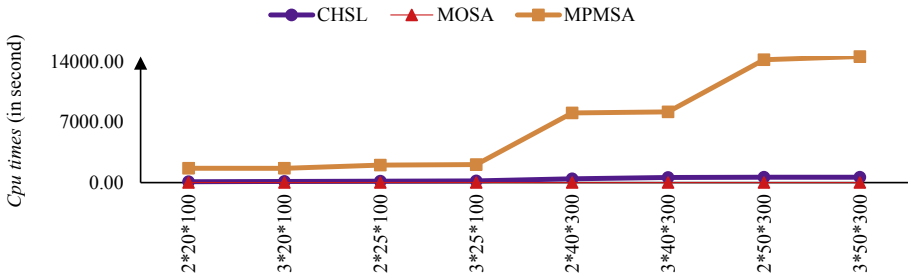

Fig. 10. *CPU time* in large-sized problems.

CPU time for different methods in large-sized problems.

In large-sized problems, ANOVA was performed on the *CPU time*. According to the results, the number of flights was the only parameter exhibiting statistically significant correlation with the *CPU time* in large-sized problems. Also, Fig. 10 confirms that the MPMSA in terms of the *CPU time* indicates the highest sensitivity to the problem size than the two other methods.

The most significant findings emerged from our paper are as follows. The trade-off between CO_2 emissions and passenger service level was addressed differently via different solution methods and problems with different dimensions. The Aug.eps found Pareto optimal solutions by spending considerable time, as confirmed by our findings. Therefore, solution methods are required that can achieve solutions as accurately as those of the Aug.eps within a reasonable time. We developed the CHSL and implemented the MOSA and MPMSA to address the need. In some measures, statistical tests found no significant differences between the Aug.eps and CHSL, while the CHSL indicated even better performance under the *SM*. The MPMSA also improved the quality of solutions compared with the MOSA by spending more time. Statistical tests revealed that the MPMSA and the CHSL lead to similar outcomes.

6. Conclusion

Our paper addresses the integration of flight scheduling, aircraft-path assignment, and gate assignment with the goal of minimizing CO_2 emissions costs and passenger service level cost. There is a trade-off between these two objectives. We develop a mathematical model to adjust the aircraft speed with the aim of balancing these conflicting objectives. The results suggest that the improvement in CO_2 emissions can be achieved by the model, but the complexity of the problem makes the model inefficient for large-sized problems. So, we offer alternatives including the development of a constructive heuristic algorithm and extending the multi-objective simulated annealing algorithm. The results show that the model can improve CO_2 emissions and passenger service level by about 11% and 31%, respectively, and the constructive heuristic performs well, as it offered acceptable results. All of the above efforts are made to improve two major concerns in airline industry: CO_2 emissions and passenger service level.

The contributions of our paper to the literature are fourfold. First, we develop a new mathematical model to make flights greener. Secondly, we use new indicators for measuring passenger service level. Third, we use various tools to reduce CO_2 emissions. Fourth, we develop a constructive heuristic algorithm, use the multi-objective simulated annealing algorithm, and extend this algorithm to enhance its performance. These contributions enrich the method of operational research in flight planning. Our findings in this paper have also made a number of significant contributions to managing airlines to improve CO_2 emissions and passenger service level.

In our future research, we intend to concentrate on the following ideas. The tools introduced in the literature review to be used for reducing CO_2 emissions for the problem stated. Other indicators for passenger service level can be considered. Other heuristic and metaheuristic algorithms can be used.

Appendix A. Problem notation

The notation of the problem is as follows:

Indexes

i,j	Index for flight
t	Index for aircraft
d	Index for day
l	Index for speed level
o	Index for gate

Parameters

F	Set of flights
T	Set of aircrafts
D	Set of planning days (dlt represents the last day in planning horizon)
L	Set of speed levels
G	Set of available gates
$N(F), N(T)$	Number of flights and aircrafts
on_i, dn_i	Origin and destination of flight i
p_{ij}	1 if flight i and flight j have passengers in common, 0 otherwise
u_{ij}	1 if destination of flight i and origin of flight j is the same, 0 otherwise
mo_{ij} (md_{ij})	1 if origin (destination) of flight i and flight j is the same, 0 otherwise
ds_i	Distance between the origin and destination of flight i
$wd_o^{on_i}$ ($wd_o^{dn_i}$)	Walking distance between gate o and entrance/exit at origin (destination) of flight i
st_d, ft_d	Start and finish times of day d
TP_{ij}	Turnaround time, time needed to connect passengers between flight i and flight j
TA_{ijt}	Turntime, time needed to prepare aircraft t between flight i and flight j
$E[NC_i]$	Expected non-cruise time for flight i
sp_{tl}	Value of speed level l for aircraft t (kilometer/minutes)
$sp_{it}^{\min}$, $sp_{it}^{\max}$	Minimum and maximum speed of aircraft t for flight i
c_{co_2}	CO2 emissions costs in kg
γ	Cruise flight time cost per hour
$Daily_t$	Daily cost when aircraft t is used
ϑ	Cost of walking per meter
τ	Constant factor for CO2 emissions per kg of fuel consumption
$bigM$	A big number

Decision variables

e_{td}	1 if aircraft t performs more than one flights on day d, 0 otherwise
σ_{td}	0 if aircraft t performs just one flight on day d, a positive random number otherwise
v_{itd}	1 if aircraft t performs flight i on day d, 0 otherwise
x_{ijtd}	1 if aircraft t performs flight i and flight j consecutively on day d, 0 otherwise
w_{itl}	1 if aircraft t performs flight i at speed level l, 0 otherwise
y_{itd}	1 if aircraft t starts day d with flight i, 0 otherwise
z_{itd}	1 if aircraft t finishes day d with flight i, 0 otherwise
$g_{io}^{on_i}$ ($g_{io}^{dn_i}$)	1 if gate o assigns to origin of flight i (destination of flight i), 0 otherwise
dp_i, ar_i	Departure and arrival times for flight i
f_{it}	Cruise time in minutes for flight i with aircraft t

References

Abdullah, M.A., Chew, B.C., Hamid, S.R., 2016. Benchmarking key success factors for the future green airline industry. Proc. Soc. Behav. Sci. 224, 246–253.
Aktürk, M.S., Atamtürk, A., Gürel, S., 2014. Aircraft rescheduling with cruise speed control. Oper. Res. 62 (4), 829–845.
Barnhart, C., Belobaba, P., Odoni, A.R., 2003. Applications of operations research in the air transport industry. Transport. Sci. 37 (4), 368–391.
Barnhart, C., Cohn, A., 2004. Airline schedule planning: accomplishments and opportunities. Manuf. Serv. Oper. Manag. 6 (1), 3–22.
Brueckner, J.K., Zhang, A., 2010. Airline emission charges: effects on airfares, service

quality, and aircraft design. Transp. Res. Part B 44 (8), 960–971.
Cavcar, A., Cavcar, M., 2004. Impact of aircraft performance differences on fuel consumption of aircraft in air traffic management environment. Aircraft Eng. Aero. Technol. 76 (5), 502–515.
Chow, C.K.W., 2014. Customer satisfaction and service quality in the Chinese airline industry. J. Air Transport. Manag. 35, 102–107.
Cui, Q., Li, Y., 2016. Airline energy efficiency measures considering carbon abatement: a new strategic framework. Transp. Res. Part D 49, 246–258.
Cui, Q., Li, Y., 2017. Will airline efficiency be affected by "Carbon Neutral Growth from 2020" strategy? Evidences from 29 international airlines. J. Clean. Prod. 164, 1289–1300.
Cui, Q., Li, Y., Yu, C.L., Wei, Y.M., 2016. Evaluating energy efficiency for airlines: an application of virtual frontier dynamic slacks based measure. Energy 113, 1231–1240.
Dalmau, R., Prats, X., 2015. Fuel and time savings by flying continuous cruise climbs: estimating the benefit pools for maximum range operations. Transp. Res. Part D 35, 62–71.
Díaz-Ramírez, J., Huertas, J.I., Trigos, F., 2014. Aircraft maintenance, routing, and crew scheduling planning for airlines with a single fleet and a single maintenance and crew base. Comput. Ind. Eng. 75, 68–78.
Duran, A.S., Gürel, S., Aktürk, M.S., 2015. Robust airline scheduling with controllable cruise times and chance constraints. IIE Trans. 47 (1), 64–83.
Engrand, P., 1998. A Multi-objective Optimization Approach Based on Simulated Annealing and its Application to Nuclear Fuel Management. Tech. Rep.. 98NB00037, Electricite de France.
EUROCONTROL, 2012. User Manual for the Base of Aircraft Data (BADA) Revision 3.10. Technical Report12/04/10-45. EEC Technical/Scientific, Eurocontrol, Eurocontrol Experimental Center, B.P. 15, F-91222 Bretigny-sur-Orge, France.
Franco, A., Rivas, D., 2014. Analysis of optimal aircraft cruise with fixed arrival time including wind effects. Aero. Sci. Technol. 32 (1), 212–222.
Fukui, H., Miyoshi, C., 2017. The impact of aviation fuel tax on fuel consumption and carbon emissions: the case of the US airline industry. Transp. Res. Part D 50, 234–253.
Gholami, S., Jalalian, M., Ramezanian, R., 2016. Exploring energy efficiency and service quality of airlines with cruise speed control. IORS 7 (1), 43–68.
Gronau, R., 1970. The effect of traveling time on the demand for passenger transportation. J. Polit. Econ. 78 (2), 377–394.
Gürkan, H., Gürel, S., Aktürk, M.S., 2016. An integrated approach for airline scheduling, aircraft fleeting and routing with cruise speed control. Transp. Res. Part C 68, 38–57.
Hagmann, C., Semeijn, J., Vellenga, D.B., 2015. Exploring the green image of airlines: passenger perceptions and airline choice. J. Air Transport. Manag. 43, 37–45.
Hu, Y., Song, Y., Zhao, K., Xu, B., 2016. Integrated recovery of aircraft and passengers after airline operation disruption based on a GRASP algorithm. Transp. Res. Part E 87, 97–112.
Hussain, R., Al Nasser, A., Hussain, Y.K., 2015. Service quality and customer satisfaction of a UAE-based airline: an empirical investigation. J. Air Transport. Manag. 42, 167–175.
Hwang, C., Yoon, K., 1981. Multiple Attribute Decision Making: Methods and Applications, a State of the Art Survey. Springer -Verlag, New York, NY.
IATA, 2010. Airline Fuel and Labor Cost Share. http://www.iata.org/. (Accessed 27 August 2017).
Jiang, H., Zhang, Y., 2016. An investigation of service quality, customer satisfaction and loyalty in China's airline market. J. Air Transport. Manag. 57, 80–88.
Kılkış, Ş., Kılkış, Ş., 2016. Benchmarking airports based on a sustainability ranking index. J. Clean. Prod. 130, 248–259.
Kurtulmuşoğlu, F.B., Can, G.F., Tolon, M., 2016. A voice in the skies: listening to airline passenger preferences. J. Air Transport. Manag. 57, 130–137.
Li, Y., Wang, Y.Z., Cui, Q., 2016. Has airline efficiency affected by the inclusion of aviation into European Union Emission Trading Scheme? Evidences from 22 airlines during 2008–2012. Energy 96, 8–22.
Mavrotas, G., 2009. Effective implementation of the ε-constraint method in multi-objective mathematical programming problems. Appl. Math. Comput. 213 (2), 455–465.
Miyoshi, C., 2014. Assessing the equity impact of the european union emission trading Scheme on an african airline. Transport Pol. 33, 56–64.
Parmentier, A., 2013. Aircraft Routing: Complexity and Algorithms, Master's Thesis. Ecole des Ponts ParisTech.
Prats, M.X., Hansen, M., 2011. Green delay programs, absorbing ATFM delay by flying at minimum fuel speed. In: Air Traffic Management Research and Development 2011, pp. 1–8.
Ryerson, M.S., Kim, H., 2014. The impact of airline mergers and hub reorganization on aviation fuel consumption. J. Clean. Prod. 85, 395–407.
Şafak, Ö., Gürel, S., Aktürk, M.S., 2017. Integrated aircraft-path assignment and robust schedule design with cruise speed control. Comput. Oper. Res. 84, 127–145.
Scotti, D., Volta, N., 2015. An empirical assessment of the CO2-sensitive productivity of European airlines from 2000 to 2010. Transp. Res. Part D 37, 137–149.
Skorupski, J., 2015. The risk of an air accident as a result of a serious incident of the hybrid type. Reliab. Eng. Syst. Saf. 140, 37–52.
Suki, N.M., 2014. Passenger satisfaction with airline service quality in Malaysia: a structural equation modeling approach. Res. Transp. Bus. Manag. 10, 26–32.
Turgut, E.T., Cavcar, M., Usanmaz, O., Canarslanlar, A.O., Dogeroglu, T., Armutlu, K., Yay, O.D., 2014. Fuel flow analysis for the cruise phase of commercial aircraft on domestic routes. Aero. Sci. Technol. 37, 1–9.
Vlachos, I., Lin, Z., 2014. Drivers of airline loyalty: evidence from the business travelers in China. Transp. Res. Part E 71, 1–17.